Experimental and Modeling Study of Abrasive Wear of Tungsten Carbide Drilling Bit in Wet and Dry Conditions

Asst. Prof .Dr. Fathi Al-Shammaa
Department of mechanical Eng.
College of Eng.
Baghdad university / Iraq
Email : fathi_alshamma@yahoo.com

Dr. Amar Hussein Al-Allaq
Department of mechanical Eng.
College of Eng.
McGill university / Canada
Email : amarallaq@mcgill.ca

Mohaimen Habeeb Makki
Lecturer in mechanical Eng
Email : mohaimen77@yahoo.com

ABSTRACT

The results of theoretical and experimental investigations carried out to study the effect of load and relative sliding speed on the abrasive wear behavior in drilling bit teeth surfaces of an insert tungsten carbide bit have been presented. Experimentally, an apparatus for abrasive wear tests conducted on the modified ASTM-G65 was modified and fabricated to facilitate loading and measurement of wear rate for the sand/ steel wheel abrasion test, which involves two cases of contact; first is at dry sand and second is under wet condition. These tests have been carried under varied operating parameters of normal load and sliding speed. A theoretical model based upon the Archard equation has been developed for predicting wear simulation by using ANSYS12.1 program for dry and wet abrasive wear rates. The general trend for all the results of wet tests is that an increase in the applied load as well as wheel rotational speed produces an increase in wear rate, while at the dry tests the behavior shows an increase and fluctuating in wear rate due to the transition in wear mechanism. As compared to the dry tests, the volume losses in wet tests have much higher values, that is because the presence of water which causes high adhesion between sand particles and specimen surface as well as wear-corrosion interaction which accelerate the wear rates. The percentage errors between theoretical and experimental results are more stable with the wet than dry tests due to the stability in wear rates.

Keywords : **abrasive wear, WC-hardmetals, archard theory, friction, ANSYS program**

دراسة عملية و نمذجة البلي بالاحتكاك لدقاق الحفر كاربيد التنجستن في الحالتين الرطبة و الجافة

د. فتحي الشماع
قسم هندسة الميكانيك
كلية الهندسة / جامعة بغداد

د. عمار العلاق
قسم هندسة الميكانيك
جامعة ميكيل/ كندا

الباحث مهيمن حبيب
اختصاص هندسة ميكانيك
جامعة بغداد

الخلاصة

انجاز النتائج النظرية والفحوصات العملية التي نفذت لدراسة تأثير الحمل وسرعة الانزلاق النسبية على تصرف البلي في سطوح الاسنان لدقاق حفر كاربيد التنجستن. عمليا ، جهاز لاختبارات البلي والذي يكون ضمن المواصفة العالمية ASTM G65 المعدلة عدّل وصُنِع لتَسهيل التحميل وقياس مدى البليان وذلك باستخدام الرملِ مع عجلةِ فولاذية للاختبار، والذي يَتضمّنُ إثنين مِنْ حالاتِ الإحتكاك؛ أولاً باستخدام الرملِ الجاف والثانيةِ تحت الشرطِ الرطبِ. هذه الإختباراتِ اجريت تحت ظروف التشغيل المختلفةِ مِنْ الحملِ المسلط والسرعةِ المنزلقةِ. كما تم استخدام نموذج نظري مطوّر مستند على معادلةِ Archard لتَوَقُّع معدلات البلي تحت التاثير الرطب والجاف بإستعمال برنامج ANSYS 12.1 . إنّ الإتجاه العامَ لكُلّ نَتائِج الإختباراتِ الرطبةِ تلك هي ان الزيادةِ في

الحملِ المسلط بالإضافة إلى سرعةِ العجلةِ التدويريةِ تُنتجُ زيادةً في معدل البلي، بينما في الإختباراتِ الجافّةِ، يشير السلوكُ الى الزيادةً والتذبذب في معدل البلي بسبب التحول في ميكانيكية التاكل. بالمقارنة مع الإختباراتِ الجافّةِ، خسائر الحجمَ في الإختباراتِ الرطبةِ لَها قِيَمُ أعلى بكثيرُ، وذلك لان وجود الماء يسبب الالتصاق العالي بين حبيبات الرمل مع سطح العينة بالاضافة الى تاثير التاكل الكيميائي والذي يُعجّلُ معدل البلي. إنّ نسبة الخطأ المئويةَ بين النَتائِجِ النظريةِ والتجريبيةِ أكثر استقراراً بالاختبارات الرطبة مِنْها في الإختباراتِ الجافّةِ وذلك بسبب الإستقرارِ في معدلات البلي.

لكلمات الرئيسية : البلي الانخلاعي ، تنجستن كاربيد معدن ذو صلابة عالية ، نظرية ارجارد ، الاحتكاك ، برنامج ANSYS 12.1

1. INTRODUCTION

Whenever surfaces move over each other, wear will occur in the form of damage to one or both surfaces, generally involving progressive loss of material. Damage-resistant surfaces are required in many engineering components to meet demanding performance requirements in contact applications. For example, in rock drilling equipment, constant rubbing action of the drilling head against the hard surfaces of rocks leads to wear and requires frequent replacement of the drilling head. In the process of design of machine elements and tools operating in contact conditions, engineers need to know areas of contact, contact stresses, and they need to predict wear of rubbing elements. These examples illustrate the critical need for new and improved materials and design methods for better wear resistant surfaces ,**Mandar Rajiv Thakare 2008.**

2. ARCHARD´S EQUATION

Archard has set his formula in 1957 and it is based on the previous work of Holm made in 1946. Archard equation is used for the analysis of wear when the deformation of the specimen is plastic. This equation gives a relation between the volume of wear, the normal load and the sliding distance. Archard´s equation is defined by,**Mandar Rajiv Thakare, 2008:**

$$Q = \frac{V}{L} = \frac{KW}{H} \quad (1)$$

Where Q is the wear rate, V is the wear volume, L is the sliding distance, K is a constant known as dimensionless wear coefficient, W is the total applied normal load and H is the surface hardness. **Mandar Rajiv Thakare, 2008** mentioned that this equation is exactly same as the Archard's equation, which was originally derived for sliding wear of metals. Tatjana Lazovic, Radivoje Mitrovic and **Mileta Ristivojevic ,2003** explained

that the surface roughness is not a factor in this measure of wear because the wear is assumed to be severe enough that surface roughness difference is insignificant.
Archard's wear equation states that the wear rate Q in any contact is directly proportional to the load applied W and inversely proportional to the

surface hardness of the wearing material H. Since the knowledge of the dimensionless wear coefficient and the hardness of the top layer of the surface may not be known with certainty, a more useful term is defined by taking the ratio K/H, which is known as the *specific wear rate* (κ, *SWR*) with the units of $mm^3N^{-1}m^{-1}$ and represents wear volume (mm^3) per unit sliding distance (m) per unit normal load (N). The modified Archard's wear equation is given by **Mandar Rajiv Thakare ,2008:**

$$\kappa = \frac{V}{WL} = \frac{K}{H} \quad (2)$$

Where V is the wear volume in mm^3, W is the total applied load in N, L is the sliding distance in m, K is the dimensionless wear coefficient and H is the surface hardness of the material.

It has been shown experimentally that the loss of material is proportional to the sliding distance except for short tests where the non-linear running-in periods are significant. However, proportionality between wear rates and normal loads is found less often. Abrupt transitions from

low to high wear rates and sometimes back again are often found with increase in load. This is due to the transition between wear mechanisms observed with change in applied loads. Also no mention has been made of the velocity of sliding or the apparent area of contact in the equation 1, suggesting that the wear rate *Q* should be independent of these factors as, **Mandar Rajiv Thakare, 2008 mentioned.**

3 .WEAR SIMULATION ANALYSIS

John M. Thompson and Mary Kathryn Thompson, 2006 put a proposal to calculate wear by using creep formula in ANSYS program.

This proposal shows that the starting point for any discussion of wear on the macro scale is the Archard equation, which states that:

$$\Delta V = \kappa \times S \times L \quad (3)$$

Where ΔV is the change in volume due to wear, L is the sliding distance, S is the normal contact stress and κ is the wear per unit pressure (or unit normal load, as in equation 2) per sliding distance. Archard says "[κ] may be described as the coefficient of wear and, in a series of experiments with the same combination of materials; changes in [κ] denote changes in surface conditions".

The Archard equation assumes that the wear rate is independent of apparent area of contact. However, it makes no assumptions about the surface topography (surface roughness effects are encompassed by the experimental wear coefficient) and it also makes no assumptions about variations with time. It must also be stated that although it is widely used, the Archard equation only provides for an order of magnitude estimate and is a true calculation of wear.

A method proposed for calculating wear is included into a finite element program where wear will be calculated in the solution processor instead of in the post processor.

Consider a modified form of the Archard equation:

$$\Delta V = \kappa \times S^{C_2} \times R_\circ^{C_3}$$

Where ΔV is the change in volume, κ, C_2 and C_3 are equation constants to account for such things as the materials in contact, S is the stress created by the contacting pair and $R_\circ$ is the number of repetitions of the load (one sliding pass, for example). If ΔV represents the change in volume of the element due to wear, then we can define wear strain as the change in volume divided by the original (initial) volume and rewrite the wear equation as:

$$e_{wr} = c_1 \times S^{c_2} \times R_\circ^{c_3} \quad (4)$$

Where e_{wr} is the wear strain, C_1 is equal to κ divided by the volume. This strain is similar to volumetric strain which has the **form**
John M. Thompson and Mary Kathryn Thompson 2006.

$$e = \Delta V / V_i = \frac{1}{3} \times (e1 + e2 + e3) \quad (5)$$

Where e1, e2 and e3 are the principal strains and V_i is the initial volume (before wear). Often only one of these strains is present for wear as it is expected that wear will occur perpendicular to the surface of the component. But that is not a requirement and wear strain may be a vector quantity in a manner similar to any other type of strain. Loads that are applied oblique to the surface may generate wear that is not perpendicular to that surface and provisions should be made for including this type of wear. The principal difference between wear strain and any other strain quantity is that wear strain represents material that is removed from the system. Wear strain as proposed here is different from wear as proposed by Archard.

The Archard equation is a systems approach where the applied load is assumed to be distributed over the entire loading area. Wear would be expected to occur uniformly over the entire surface. The wear strain proposed here is a function stress and load repetitions. This implies that where load is applied to the surface, wear will occur and that parts of the surface which are currently unloaded will not experience change due to wear. This definition of wear strain also considers the local effect of stress and permits wear to be different at different locations on the surface. This does not change the fact that the approach presented here is only a systems level estimate of the wear and that

detailed calculations at specific locations on a surface should not be relied upon.
This form of the wear equation, **Eq. 4**, is similar to creep equations that have a material constant (C_1), a stress contribution (S and C_2) and a third factor, creep strain or time in the case of creep equation and repetitions in the case wear. This suggests that creep may be used to simulate wear until such time as wear is directly calculable in ANSYS. Explicit creep is used since the plan is to calculate the wear strain based upon the final configuration of the surface at the end of the load step. In ANSYS, the explicit creep calculation is performed after the elastic and plastic calculations are completed; this is the approach used for wear. The strain hardening creep equation that is programmed into ANSYS has the form:

$$de_{cr}/dt = c_1 \times \text{stress}^{c_2} \times e_{cr}^{c_3} \times \exp(-c_4/T) \quad (6)$$

Where C_1,C_2, C_3 and C_4 are constants that are supplied by the user. For each time increment, the incremental creep strain is calculated using this equation, then incremental creep strain is multiplied by the incremental time and added to the previous creep strain. A similar procedure can be used to calculate wear. The incremental wear strain can be calculated in a similar manner. For each load step, the incremental wear strain is calculated multiplied the load step time and added to the previous wear strain.

4. CALCULATION OF FRICTION FORCE

We derived a mathematical model, as explained below, to calculate the friction force from the difference in electrical power absorbed before and after the contact between the specimen and the rotating wheel (ΔP) which is taken from a three phase powermeter device.

$$\Delta P = P_2 - P_1 = \Delta t_r \times \Omega \quad (7)$$

$$\Omega = \frac{2\pi N}{60}$$

$$F_f = \frac{\Delta t_r}{R} = \frac{\Delta P/\Omega}{R} = \frac{60\,\Delta P}{2\pi N R} \quad (8)$$

Where F_f is the friction force (N), Δt_r variation in torque (N.m), R radius of rotating wheel (m), ΔP variation in power absorbed (watt), Ω angular velocity of the rotating wheel (rad/sec), N revolution per minute (rpm) for the rotating wheel, P_1 power absorbed before the contact and P_2 is the power absorbed after the contact.

5 .COEFFICIENT OF FRICTION

The friction force is the resisting force tangential to the interface between two bodies when, under the action of an external force, one body moves or tends to move relative to the other and the coefficient of friction is the ratio of the force resisting tangential motion between two bodies (F_f) to the total applied normal load (W), the definition is represented by the following equation.

$$COF = \frac{F_f}{W} \quad (9)$$

Also it is an appropriate way to describe the resistance to relative motion between surfaces, but it is not a material property, nor is it a physical constant like the speed of light in a vacuum or Avogadro's number or the elementary charge on the electron as mentioned, by **Ameer Hussein Ali 2008.**

6 .EXPERIMENT

6.1 Experimental Material

The samples are teeth which were taken from an insert tungsten carbide $8_{1/2}$" tri-cone drilling bit. The specimen considered has a cone of 6.78 mm bottom radius and 3.5 mm upper radius and depth of 1mm with cylindrical base of 6.78 mm radius and 20 mm height, **Fig. 17a**. The area of contact (A) is equal to (πr_i^2), r_i= 3.5 mm, and then A= 38.48 mm^2. The roughness (Ra) of the contact surfaces is found to be Ra = 5.583 to 7.808 µm.

6.2 Materials Properties

X-ray diffraction (XRD) test shows that the material of the tooth is based upon WC-based hardmetal; by X-ray fluorescence (XRF) test, it was observed that the specimen contain Pt (11.2646%) and Ni (0.7253%). And from micro hardness test we found that the average hardness of the tooth is 1532 HV. Also it was found that

the Young's modulus (E) of tooth material can be 601 Gpa. The density of the samples' material is calculated by taking a piece of sample and weighting it, then by using a tube and filling it with water and then pull out the water to know its volume, after that we put the piece of the sample in the tube and filling it again with the water and then pull out the water to know its volume, the difference in water volume before and after putting the sample´s piece in the tube represents the sample´s piece volume, then by dividing sample´s piece weight on its volume to get the density of the sample´s material which was found to be 13.3 g/cm^3.The average microhardness of the steel wheel is 271.15 HV.

6.3 Test Apparatus

Abrasive wear tests were performed using the steel wheel high abrasion stress with diameter of 229 mm. The test set-up of the modified ASTM-G65 test is shown in figure 1. Basically, this standard uses the rubber wheel as the counterface, K. Elalem and D.Y. Li 2001, and this case of contact known as "low abrasion stress". Some researchers used both the rubber wheel and steel wheel for their studies ,**Wirojanupatump and Shipway 2000**. The wheel is driven by a nominally 1.4 kW (2 hp) AC motor through a 10/1 gear box to ensure that full torque is delivered during the test. The abrasives are fed between the wheel and the sample from a hopper by a nozzle. The sample is pressed against the wheel by a loaded lever. The test is run for a set period and the wear is measured by calculating the volume of material lost through weight loss and density measurements. Silica sand of 1mm, as maximum size, is used as abrasives during these tests. The machine shall be equipped with a revolution counter that will monitor the number of wheel revolutions as specified. It is recommended that the incremental counter have the ability to shut off the machine after a preselected number of wheel revolutions.

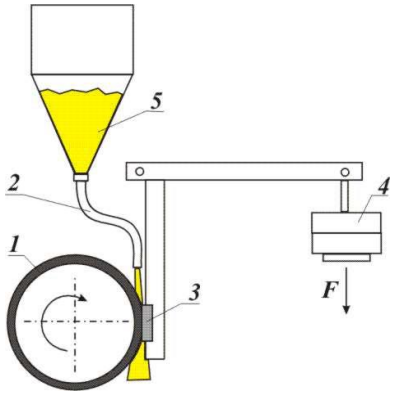

Figure 1. Schematic representation of the test apparatus.

The test apparatus mainly consists from the following parts, **Fig. 1**:

1. The wheel.

2. Sand nozzle.

3. Specimen Holder and Lever Arm

4. Applied weight.

5. Sand hopper.

6.4 Test Procedure

The test time is selected to be as 15 minute. The speeds of rotation for the wheel were selected to be 160 rpm, 220 rpm and 300 rpm. The effective applied load and contact pressure at each rotating speed are illustrated in **Table 1**. The abrasives flow rate which was used in dry tests**, Fig. 16a** was 350 g/min and of 200 g/min in wet tests, **Fig. 16b**, with water flow rate of 125 g/min. When the wheel rotation will be started, the lever arm automatically will be lowered to allow the specimen to contact the wheel. When the test has run at the desired time, the specimen automatically will be lifted away from the wheel and then we have to stop the sand/slurry flow and wheel rotation. The abrasive wear was determined from the mass loss results, which were measured with 0.001 g resolution, converted to volume loss by the following equation:

$$\text{Volume loss (mm}^3) = \frac{\text{mass loss (g)}}{\text{density } (\frac{\text{g}}{\text{cm}^3})} \times 1000 \qquad (10)$$

7. RESULTS AND DISCSSION

7.1 Wear Performance

The effects of the effective applied load on the performance characteristics of wear rates were examined by analyzing five different weights during each rotational speed. The graphs of applied pressure versus wear volume loss are shown in **Figs. 2** and **3**. It shows at dry tests that there was a fluctuating in the volume loss as the applied load was increased, but more stability in wear volumes at wet tests. A phenomenon was observed by A.J. **Gant and M.G. Gee 2001 and X. Ma, R. Liu and D.Y. Li 2000** on the wear loss of D2 steel by ASTM-G65 device using silica sand as abrasive material. It shows that the damage to the abrasive sand particles was markedly increased at the higher sliding speed. The severe damage to the abrasive sand explains why at higher sliding speeds, the volume loss of the samples was lower than that at lower sliding speeds. This happened because the relatively brittle SiO_2 sand could not withstand increased impact at higher sliding speeds when interacted with hard but relatively tougher D2 steel. Generally, under higher loads, the damage to the sand particles considerably increased, leading to less wear of the sample. This reason explains the variations in the relation between the wear losses of the tested materials and the applied load. The damage to sand under high loads was so high that a decrease in the volume loss of the target material could occur as the applied load was increased.

The same reason above can be suggested as one reason responsible for the decreasing in volume loss as the sliding speed or the applied load was increased.

The results of COF versus load with dry and wet tests at each rotational speed are illustrated in **Figs. 4** and **5.** Generally, the COF have the highest values at 220 rpm at the dry and wet tests. Friction, through a heating effect, can affect material properties, which in turn can influence wear behavior. In addition, friction modifies the contact stress system by introducing a shear or traction component, which can also be a factor in wear behavior. Because of these aspects, friction and wear must be generally considered as related phenomena, but not equivalent phenomena, **Raymond G. Bayer, 2004**. The general trend is that the behavior of the COFs shows a fluctuating response with respect to the applied pressure as well as to the wheel rotational speed due to the transition in wear mechanism.

Figs. 6 and **7** illustrate the temperature evaluations along with cases of contact by using laser thermometer. These temperatures represent the maximum values obtained at the end of the test time. It shows that the temperatures have the highest values at dry tests and it is proportional to the applied load and sliding speeds. Comparison between dry and wet tests, it was observed that at wet tests the temperatures have less sensitive to the applied load, which was happened due to the use of water during these tests.

Figs. 8 and **9** illustrate the SWRs behavior. At the dry tests wear coefficients or the specific wear rates (SWRs) have fluctuating values as the applied load increased and its values are decreased with an increase in the sliding speed at most loads levels. While at the wet tests the SWRs are proportional to the sliding speed and have its highest values at the minimum applied load. That is due to probability damage to the sand particles which is increasing as the applied load increased as well as increasing in the relative sliding speed. Transition in wear mechanism can produce such behavior. Comparisons between dry and wet tests we observed that the wear coefficients or SWRs are much higher at the wet than dry tests; this is due to the wear-corrosion interaction effects which can accelerate the volumes losses. Another factor can influence the volume losses during wet tests that the presence of water produces high cohesion between sand particles and high adhesion between the specimen and those particles which were accumulated above the contact surface and fall down slowly. The SWRs were calculated according to the equation ($V = k\ W$) at each effective applied load. Where V is the wear

volume loss per unit sliding distance (mm^3/m), *k* is the SWR ($\frac{mm^3}{N}/m$) and W is the total applied normal load (N). Also it was observed that the grooves created at the worn surface of the specimen are more clearly at wet tests than dry ones, **Figs. 17b** and **17c**, that is happened due to the difference in wear mechanism between them.

7.2 Simulation Results

The ANSYS program is used to simulate the wear results by using explicit creep equation. Explicit creep equation uses the wear strain phenomenon to describe the wear rate behavior. The experimental wear strains are calculated by dividing the wear volume loss, **Eq. 10**, by V_i value supposed volume before wear. Simulation wear strain and experimental wear strain results versus applied pressures are plotted as shown in **Figs. 10 to 15**. The percentage errors (PE) have been taken between the simulation results and a linear fitting to the experimental ones. Fluctuating in wear rates at the dry tests has large effects on the PE values. Very high PE over experimental in case of dry sand-300 rpm as well as at dry sand - 200 rpm are supposed to be caused by the damage in abrasive sand particles which reduces the wear loss of the specimen. Stability of wear rates at wet tests has direct effect on the stability of PE as compared to the dry ones.

8 . CONCLUSIONS

The main task of this work is to investigate the wear behavior of an insert tungsten carbide tooth material under the dry and wet sand / steel wheel abrasion conditions, and in particular, the responses of the materials to variations in the applied load and the sliding speed. It was demonstrated by the abrasion tests that the tested material showed different responses to the variations in the applied load and the sliding speed.

1. The abrasive wear rate was generally proportional to load, that is an increase in the applied load / pressure produces an increase in wear rate of the bit tooth in both dry and wet conditions.

2.The general trend for all the results of wet tests is that an increase in wheel rotational speed produces an increase in wear rate of the bit tooth. Compared in dry tests, the wear rate is decreased.

3. The abrasive wear rates were significantly altered by the presence of an aqueous carrier. High adhesion and wear-corrosion interaction produced high wear rates; it is observed that the wear coefficients (SWRs) in wet tests were approximately 10 times higher than those in the dry condition.

4. Presence of water have no effects at the COFs as compared between dry and wet tests at the rotational speeds of 160 and 220 rpm. Variations to the COFs are observed at the speed of 300 rpm, that the COFs are higher in wet than dry tests after the applied load of 64.525 N.

5. It is possible to analyze the wearing phenomenon by using ANSYS program. The percentage errors have more stability at the wet tests than dry ones due to the stability in wear rates.

9. REFERENCES

A.J. Gant and M.G. Gee ,2001, *Wear of Tungsten Carbide–Cobalt Hardmetals and Hot Isostatically Pressed High Speed Steels under Dry Abrasive Conditions*, Wear 908–915.

Ameer Hussein Ali ,2008, *Using Universal Material Tester to Study Effect of the Porosity on Wear Behavior*, Master Thesis, University of Baghdad.

G. Raymond Bayer ,2004, *Mechanical Wear Fundamentals*, Second Edition, Vestal, New York.

K. Elalem and D.Y. Li 2001, *Variations in Wear Loss with Respect to Load and Sliding Speed under Dry Sand/Rubber-Wheel Abrasion Condition: A Modeling Study* , Wear 59–65.

Mandar Rajiv Thakare, 2008, *Abrasion-Corrosion of Downhole Drill Tool Components*, Ph.D. Thesis, University of Southampton.

M.John Thompson and Mary Kathryn Thompson ,2006, *A Proposal for the Calculation of Wear*, Mechanical Engineering Dept, MIT G. Raymond

Bayer, 2004, *Mechanical Wear Fundamentals*, Second Edition, Vestal, New York.

S. Wirojanupatump and P.H. Shipway, 2000, *Abrasion of Mild Steel in Wet and Dry Conditions with the Rubber and Steel Wheel Abrasion Apparatus*, Wear 91–101.

Tatjana Lazovic, Radivoje Mitrovic and Mileta Ristivojevic, 2003, *Influence of Abrasive Particle Geometry and Material on the Abrasive Wear Mode*, University of Belgrade.

X. Ma, R. Liu and D.Y. Li, 2000, *Abrasive Wear Behavior of D2 Tool Steel with Respect to Load and Sliding Speed under Dry Sand/Rubber Wheel Abrasion Condition*, Wear 79–85.

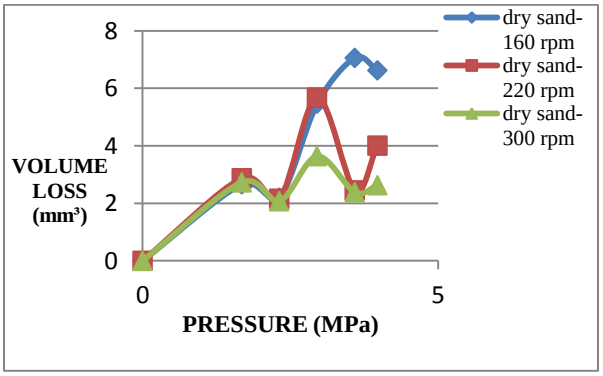

Figure 2. Overall plot of volume loss versus pressure applied in three cases of contact represent dry sand tests of 160, 220 and 300 rpm wheel rotational speeds.

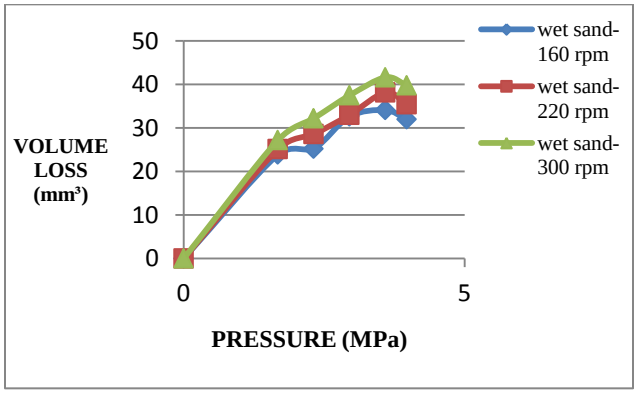

Figure 3. Overall plot of volume loss versus pressure applied in three cases of contact represent wet sand tests of 160, 220 and 300

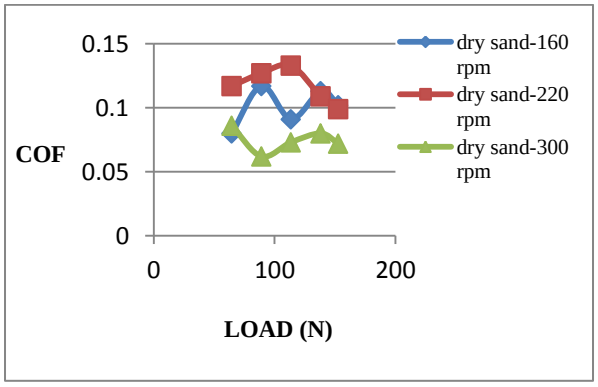

Figure 4. Overall plot of coefficient of friction versus applied load represent dry contact at 160, 220 and 300 rpm wheel rotational speeds.

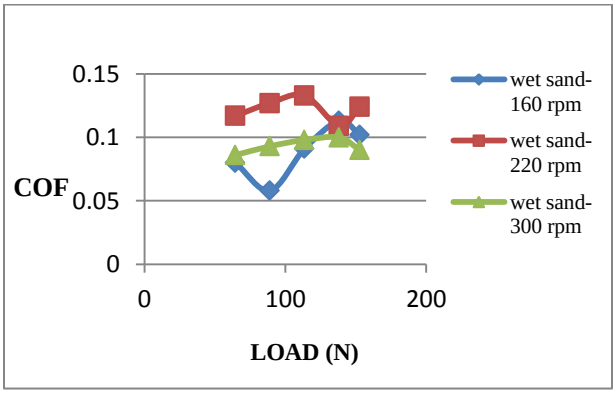

Figure 5. Overall plot of coefficient of friction versus applied load represent wet contact at 160, 220 and 300 rpm wheel rotational speeds.

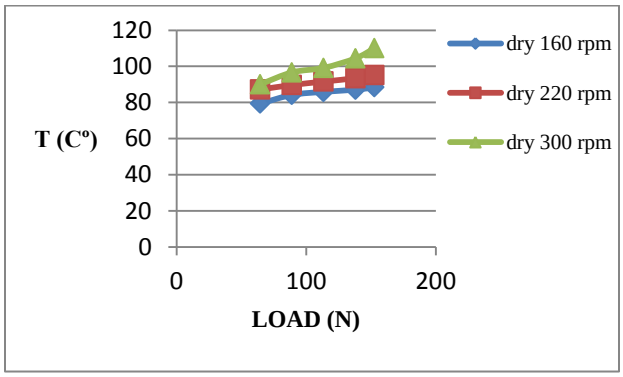

Figure 6. Comparisons of temperatures were evaluated at 160, 220 and 300 rpm wheel rotational speeds /dry condition.

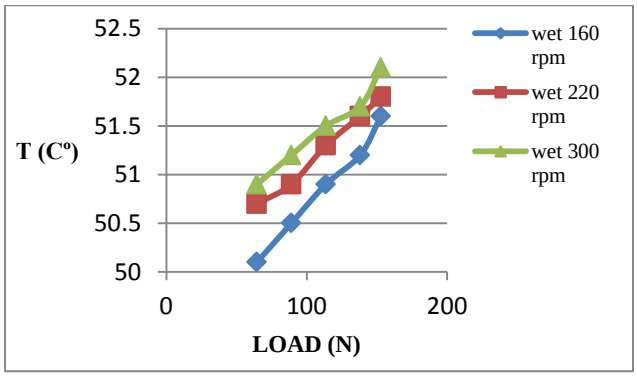

Figure 7. Comparisons of temperatures were evaluated at 160, 220 and 300 rpm wheel rotational speeds /wet condition.

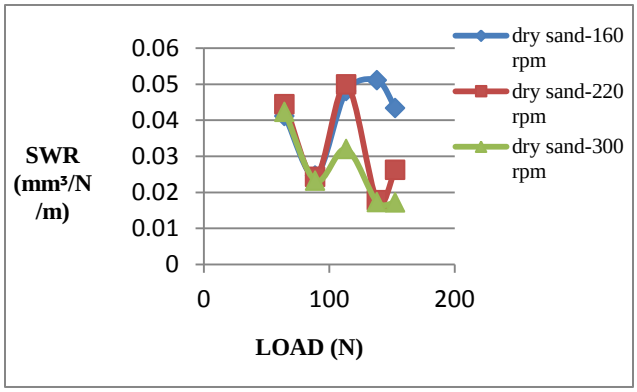

Figure 8. Comparisons of specific wear rates were evaluated at dry condition among 160, 220 and 300 rpm wheel rotational speeds.

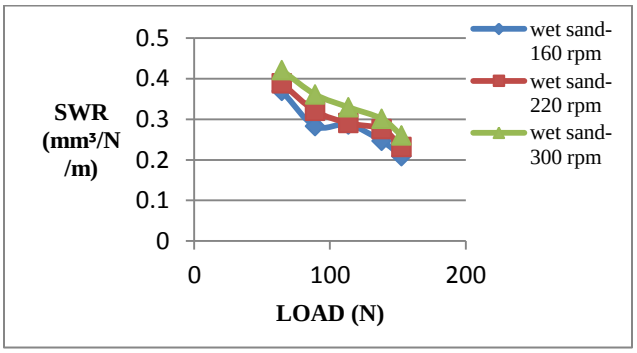

Figure 9. Comparisons of specific wear rates were evaluated at wet condition among 160, 220 and 300 rpm wheel rotational speeds.

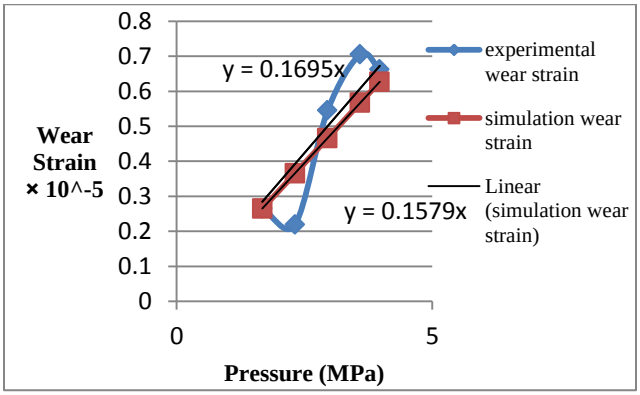

Figure 10. Plot of experimental wear strain and simulation wear strain versus applied pressure at dry sand condition and 160 rpm wheel rotational speed.

$$\text{Percentage error (PE)} = \frac{|y_{experimental} - y_{simulation}|}{y_{experimental}} \times 100\% \quad (11)$$

$$PE_{dry-160\ rpm} = \frac{|0.1695 - 0.1579|}{0.1695} \times 100\% = 6.843\%$$

(under experimental).

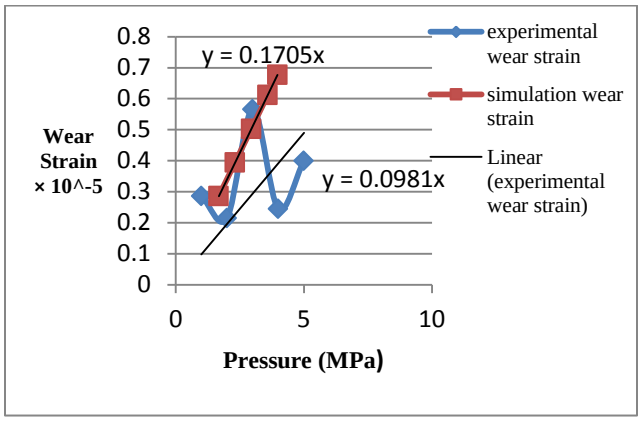

Figure 11. Plot of experimental wear strain and simulation wear strain versus applied pressure at dry sand condition and 220 rpm wheel rotational speed.

$$PE_{dry-220\ rpm} = \frac{|0.0981-0.1705|}{0.0981} \times 100\% = 73.802\ \%$$ (over experimental).

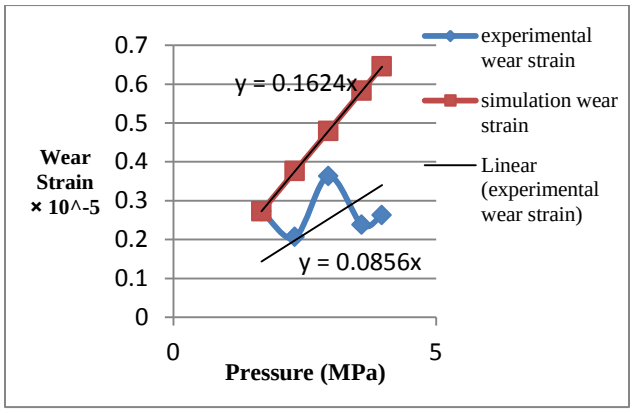

Figure 12. Plot of experimental wear strain and simulation wear strain versus applied pressure at dry sand condition and 300 rpm wheel rotational speed.

$$PE_{dry-300\ rpm} = \frac{|0.0856-0.1624|}{0.0856} \times 100\% = 89.719\%$$ (over experimental).

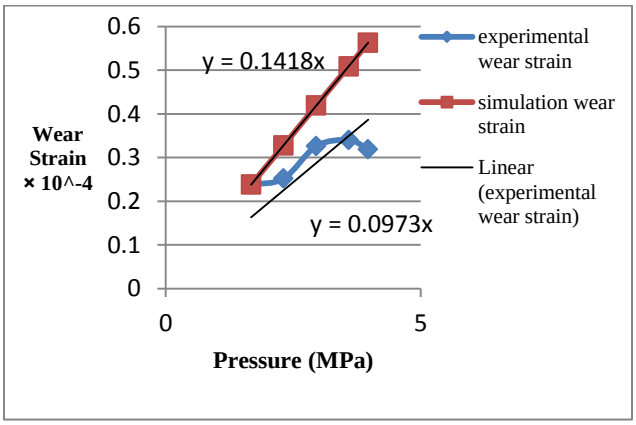

Figure 13. Plot of experimental wear strain and simulation wear strain versus applied pressure at wet sand condition and 160 rpm wheel rotational speed.

$$PE_{wet-160\ rpm} = \frac{|0.0973-0.1418|}{0.0973} \times 100\% = 45.734\%$$ (over experimental).

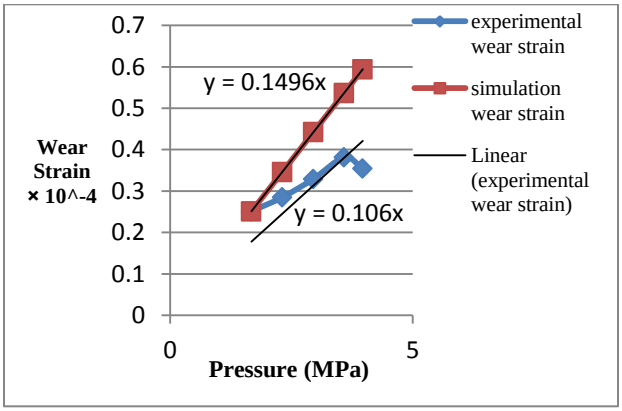

Figure 14. Plot of experimental wear strain and simulation wear strain versus applied pressure at wet sand condition and 220 rpm wheel rotational speed.

$$PE_{wet-220\ rpm} = \frac{|0.106-0.1496|}{0.106} \times 100\% = 41.132\%$$ (over experimental).

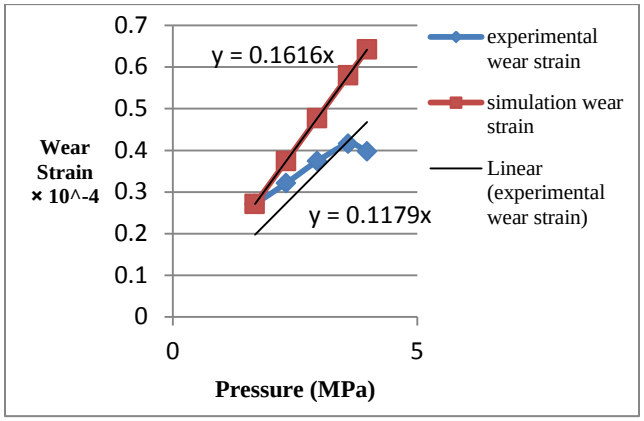

Figure 15. Plot of experimental wear strain and simulation wear strain versus applied pressure at wet sand condition and 300 rpm wheel rotational speed.

$$PE_{wet-300\ rpm} = \frac{|0.1179-0.1616|}{0.1179} \times 100\% = 37.065\% \quad \text{(over experimental).}$$

Table 1. The effective applied loads and contact pressures with respect to rotational speeds associated at each contact condition.

Contact condition	Wheel rotational speed (rpm)	Effective applied Load (N)	Contact pressure (MPa)
Dry sand/ Wet sand	160	64.525	1.676845
	220	89.05	2.314189
	300	113.575	2.951533
		138.1	3.588877
		152.815	3.971283

(a)

(b)

Figure 16. (a) -The dry sand test and (b) –The wet sand test.

(a) **(b)** **(c)**

Figure 17. Contact surface; (a) - before the test, (b) - after dry test and (c) - after wet test, (b) and (c) are at load of 138.1 N and 300 rpm.